# Supporting Information for

## Designed construction of two new atom-precise three-dimensional and two-dimensional $Ag_{12}$ cluster-assembled materials

*Riki Nakatani,*[a] *Jin Sakai,*[a] *Aishik Saha,*[b] *Ayumu Kondo,*[a] *Rina Tomioka,*[a] *Tokuhisa Kawawaki,*[a] *Saikat Das**[a] *and Yuichi Negishi**[a,c]

[a]Department of Applied Chemistry, Faculty of Science, Tokyo University of Science, Kagurazaka, Shinjuku-ku, Tokyo 162-8601, Japan.

[b]Department of Metallurgical Engineering and Materials Science, Indian Institute of Technology Bombay, Mumbai 400 076, India.

[c]Research Institute for Science & Technology, Tokyo University of Science, Tokyo 162-8601, Japan.

*Correspondence to: saikatdas@rs.tus.ac.jp (S.D.), negishi@rs.tus.ac.jp (Y.N.)

**Table of Contents**

## Materials and methods

### Materials

All starting materials and solvents were obtained from commercial sources and utilized directly as received without further purification, unless otherwise noted. *tert*-butyl mercaptan was obtained from Tokyo Chemical Industry Co., Ltd. Silver trifluoroacetate ($CF_3COOAg$) was obtained from FUJIFILM Wako Pure Chemical Corporation. Silver nitrate ($AgNO_3$), methanol, dimethylacetamide (DMAc), dimethylformamide (DMF), acetonitrile, and ethanol were obtained from Kanto Chemical Co., Inc. tris(pyridine-4-ylmethyl)amine (TPMA) and 1,3,5-tris(pyridine-4-ylethynyl)benzene (TPEB) were obtained from ET Co., Ltd.

### Methods

Single-crystal X-ray diffraction (SCXRD) was conducted for gathering the data about the single crystal, which was first immersed in cryoprotectant Parabar 10312 (Hampton Research, 34 Journey, Aliso Viejo, CA 92656-3317 USA) followed by mounting on a Dual-Thickness MicroMounts™ (MiTeGen, LLC, Ithaca, NY, USA). A Bruker D8 QUEST diffractometer was utilized for performing SCXRD measurement for **TUS 6** by subjecting the sample to a monochromatic Mo Kα radiation (λ = 0.71073 Å). Regarding **TUS 7**, SCXRD was carried out on a Rigaku XtaLaB Synergy-DW diffractometer equipped with monochromatic Cu Kα radiation (λ = 1.5418 Å). The crystal structures were determined and solved by employing the Apex4 Bruker software[1] and CrysAlis$^{Pro}$ software[2]. Powder X-ray diffraction (PXRD) patterns were procured on a Rigaku MiniFlex 600 X-ray diffractometer with a Cu Kα source (λ = 1.5418 Å) under an applied voltage of 40 kV and current of 15 mA. The range of diffraction angle $2\theta$ was 3-40º over which the intensity peaks were recorded with a step size of 0.01º and scan speed of 3.7º/min. X-ray photoelectron spectroscopy (XPS) spectra were collected on a JPS-9030 electron spectrometer (JEOL, Tokyo, Japan) utilizing a Mg Kα radiation (1253.6 eV). All the binding energies were referenced to the neutral C 1s peak at 283.3 eV. An Olympus SZX7 stereo microscope was utilized to record the optical microscope images. Scanning electron microscopy/energy-dispersive X-ray spectroscopy (SEM-EDX) was carried out for high resolution imaging/elemental mapping on a JEOL JSM-IT800SHL field emission scanning electron microscope. The thermal stability of the SCAMs were probed by thermogravimetric analysis (TGA) on a Bruker TG-DTA2010SA thermal analyzer from room temperature to 800

ºC at a heating rate of 10 ºC $min^{-1}$ under $N_2$ atmosphere. Diffuse reflectance spectroscopy (DRS) was accomplished on a JASCO V-670 spectrophotometer. The photoluminescence (PL) spectra were recorded on a SHIMADZU RF-6000 spectrofluorometer.

**Synthesis methods**

**Synthesis of silver *tert*-butylthiolate (AgS$^t$Bu).** AgS$^t$Bu was synthesized following previous reports.[3,4]

**Synthesis of TUS 6**

$[AgS^tBu]_n$ (20 mg, 0.10 mmol) and $CF_3COOAg$ (22 mg, 0.10 mmol) were mixed together in DMAc (5 mL) under stirring until the solution was transparent. On the other hand, TPMA (15.3 mg, 0.05 mmol) linker was dissolved in another glass vial that contained DMAc (1 mL). This solution was added dropwise to the inorganic solution. After leaving for 1 day in the dark, **TUS 6** (21.9 mg) was obtained in 40.6% yield on the basis of Ag as colourless octahedral-shaped crystals from the bottom of the solution.

**Synthesis of TUS 7**

To a solution of EtOH/MeCN (v/v=1:1) (5 mL) was added $[AgS^tBu]_n$ (24 mg, 0.12 mmol) and $CF_3COOAg$ (24 mg, 0.12 mmol), and the mixture was stirred vigorously until the solution became transparent. On the other hand, TPEB (11.8 mg, 0.03 mmol) linker was dissolved in another glass vial that contained DMF (5 mL). This solution was added dropwise to the inorganic solution. After leaving for 1 day in the dark, **TUS 7** (35.2 mg) was obtained in 69.6% yield on the basis of TPEB as colourless octahedral-shaped crystals from the bottom of the solution.

**Table S1.** Crystallographic parameters of **TUS 6**.

| Identification code | **TUS 6** |
|---|---|
| Empirical formula | $C_{36}H_{45}Ag_6F_9N_4O_6S_3$ |
| CCDC number | 2373129 |
| Formula weight | 1616.22 |
| Temperature/K | 273.15 |
| Crystal system | Orthorhombic |
| Space group | *Pbca* |
| a/Å | 21.868(3) |
| b/Å | 22.557(3) |
| c/Å | 22.892(3) |
| α/° | 90 |
| β/° | 90 |
| γ/° | 90 |
| Volume/Å$^3$ | 11292(3) |
| Z | 8 |
| $\rho_{calc}$/g cm$^{-3}$ | 1.901 |
| μ/mm$^{-1}$ | 2.229 |
| F(000) | 6304 |
| Crystal size/mm$^3$ | 0.24 × 0.22 × 0.2 |
| Radiation | MoKα (λ = 0.71073) |
| 2Θ range for data collection/° | 2.070 to 24.713° |
| Index ranges | -25≤h≤25, -25≤k≤26, -24≤I≤26 |
| Reflections collected | 76830 |
| Independent reflections | 9365 [$R_{int}$ = 0.2248] |
| Data/restraints/parameters | 9365 / 506 / 586 |
| Goodness-of-fit on $F^2$ | 0.968 |
| Final R indexes [I>=2σ (I)] | $R_1$= 0.0530, w$R_2$ = 0.0978 |
| Final R indexes [all data] | $R_1$ = 0.1019, w$R_2$ = 0.1157 |
| Largest diff. peak/hole / e Å$^{-3}$ | 1.565 / -0.843 |

**Table S2.** Crystallographic parameters of **TUS 7**.

| Identification code | **TUS 7** |
|---|---|
| Empirical formula | $C_{15}H_{14}Ag_2F_3NO_2S$ |
| CCDC number | 2373236 |
| Formula weight | 614.17 |
| Temperature/K | 273.15 |
| Crystal system | Trigonal |
| Space group | *R*-3 |
| a/Å | 24.5604(4) |
| b/Å | 24.5604(4) |
| c/Å | 21.6065(6) |
| α/° | 90 |
| β/° | 90 |
| γ/° | 120 |
| Volume/Å$^3$ | 11287.2(5) |
| Z | 18 |
| $\rho_{calc}$/g cm$^{-3}$ | 1.626 |
| μ/mm$^{-1}$ | 13.672 |
| F(000) | 5454 |
| Crystal size/mm$^3$ | 0.16 × 0.16 × 0.16 |
| Radiation | MoKα (λ = 0.71073) |
| 2Θ range for data collection/° | 2.915 to 74.530° |
| Index ranges | -30≤h≤22, -16≤k≤30, -21≤I≤26 |
| Reflections collected | 12388 |
| Independent reflections | 4922 [$R_{int}$ = 0.0239] |
| Data/restraints/parameters | 4922 / 184 / 220 |
| Goodness-of-fit on F$^2$ | 1.070 |
| Final R indexes [I>=2σ (I)] | $R_1$ = 0.0379, $wR_2$ = 0.1049 |
| Final R indexes [all data] | $R_1$ = 0.0417, $wR_2$ = 0.1076 |
| Largest diff. peak/hole / e Å$^{-3}$ | 0.822 / -0.951 |

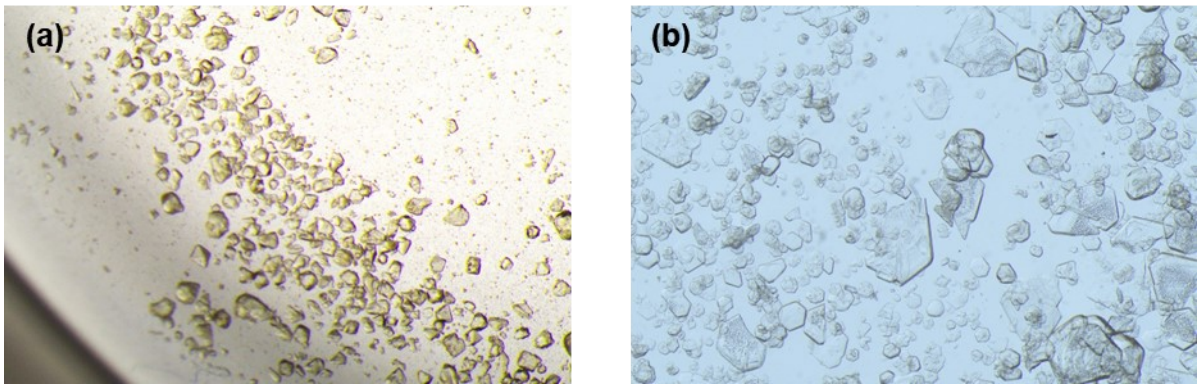


**Fig. S1** Optical microscope images of (a) **TUS 6** and (b) **TUS 7**.

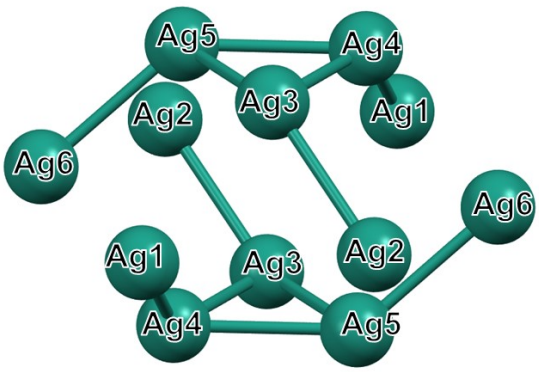


**Fig. S2** $Ag_{12}$ core architecture of **TUS 6**.

**Table S3.** Ag–Ag bond lengths for the $Ag_{12}$ hollow cuboctahedron illustrated in Fig. S2.

| Atom1 | Atom2 | Bond length/Å | | Bond length/Å |
|---|---|---|---|---|
| Ag1 | Ag4 | 3.016 | **Maximum** | 3.044 |
| Ag2 | Ag3 | 3.044 | **Minimum** | 2.936 |
| Ag3 | Ag4 | 2.961 | **Average** | 2.985 |
| Ag3 | Ag5 | 2.936 | **S.D.** | 0.042 |
| Ag4 | Ag5 | 2.954 | | |
| Ag5 | Ag6 | 3.001 | | |

**Table S4.** Ag–Ag–Ag bond angles corresponding to Fig. S2.

| Atoms | Angle/° |
|---|---|
| Ag1-Ag4-Ag3 | 137.8 |
| Ag1-Ag4-Ag5 | 100.66 |
| Ag2-Ag3-Ag4 | 99.89 |
| Ag2-Ag3-Ag5 | 136.93 |
| Ag3-Ag4-Ag5 | 59.53 |
| Ag3-Ag5-Ag4 | 60.34 |
| Ag4-Ag3-Ag5 | 60.13 |
| Ag3-Ag5-Ag6 | 100.62 |
| Ag4-Ag5-Ag6 | 137.63 |

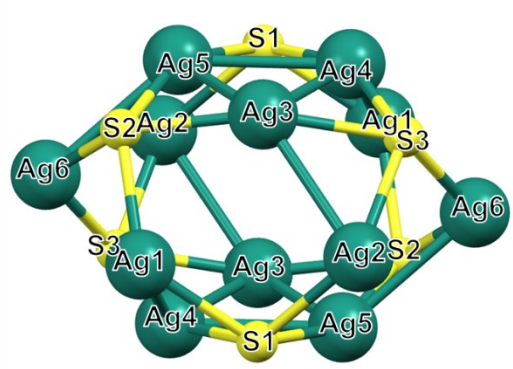


**Fig. S3** Attachment of six thiolates on the $Ag_{12}$ cluster node in **TUS 6**.

**Table S5.** Ag–S bond lengths corresponding to Fig. S3.

| Atom1 | Atom2 | Bond length/Å | | Bond length/Å |
|---|---|---|---|---|
| Ag1 | S1 | 2.538 | **Maximum** | 2.538 |
| Ag1 | S2 | 2.511 | **Minimum** | 2.476 |
| Ag2 | S1 | 2.521 | **Average** | 2.504 |
| Ag2 | S3 | 2.537 | **S.D.** | 0.023 |
| Ag3 | S2 | 2.480 | | |
| Ag3 | S3 | 2.490 | | |
| Ag4 | S1 | 2.485 | | |
| Ag4 | S3 | 2.476 | | |
| Ag5 | S1 | 2.480 | | |
| Ag5 | S2 | 2.491 | | |
| Ag6 | S2 | 2.522 | | |
| Ag6 | S3 | 2.520 | | |

**Table S6.** Ag–S–Ag and Ag–Ag–S bond angles corresponding to Fig. S3.

| Atoms | Angle/° | Atoms | Angle/° |
|---|---|---|---|
| Ag1-S1-Ag2 | 95.55 | Ag2-Ag3-S3 | 53.46 |
| Ag1-S1-Ag4 | 73.78 | Ag4-Ag3-S3 | 53.19 |
| Ag2-S1-Ag5 | 83.96 | Ag5-Ag3-S2 | 53.96 |
| Ag4-S1-Ag5 | 73.02 | Ag2-Ag3-S2 | 119.11 |
| Ag1-S2-Ag3 | 84.49 | Ag1-Ag4-S1 | 53.91 |
| Ag3-S2-Ag5 | 72.40 | Ag3-Ag4-S3 | 53.62 |
| Ag5-S2-Ag6 | 73.53 | Ag1-Ag4-S3 | 119.71 |
| Ag1-S2-Ag6 | 94.62 | Ag5-Ag4-S1 | 53.42 |
| Ag2-S3-Ag3 | 74.51 | Ag3-Ag5-S2 | 53.64 |
| Ag2-S3-Ag6 | 94.50 | Ag6-Ag5-S2 | 53.72 |
| Ag3-S3-Ag4 | 73.19 | Ag6-Ag5-S1 | 119.36 |
| Ag4-S3-Ag6 | 83.31 | Ag4-Ag5-S1 | 53.56 |
| S1-Ag1-Ag4 | 52.31 | Ag5-Ag6-S2 | 52.75 |
| S1-Ag1-S2 | 117.56 | Ag5-Ag6-S3 | 89.51 |
| Ag4-Ag1-S2 | 89.35 | S2-Ag6-S3 | 118.79 |
| Ag3-Ag2-S1 | 88.67 | | |
| Ag3-Ag2-S3 | 52.03 | | |
| S1-Ag2-S3 | 117.33 | | |

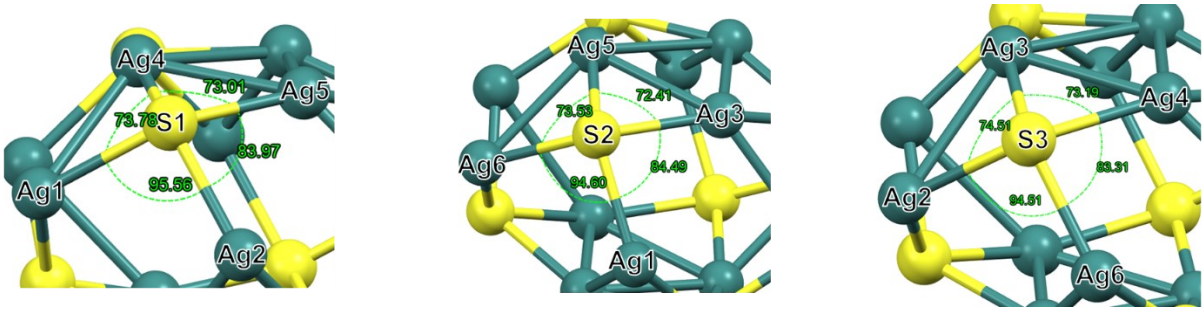


**Fig. S4** Connectivities of six S atoms that belong to S$^t$Bu molecules and constructing the cluster nodes with four different Ag atoms in $\mu_4$-$\eta^1$, $\eta^1$, $\eta^1$, $\eta^1$ ligation in **TUS 6**.

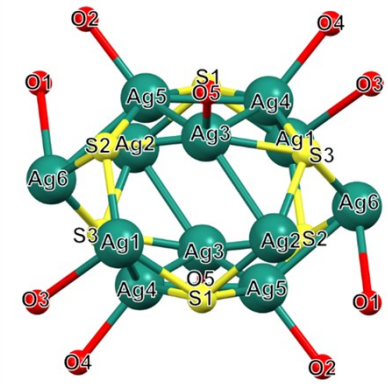


**Fig. S5** Attachment of six trifluoroacetates on the $Ag_{12}S_6$ cluster node in **TUS 6**.

**Table S7.** Ag–O bond lengths corresponding to Fig. S5.

| Atom1 | Atom2 | Bond length/Å | | Bond length/Å |
|---|---|---|---|---|
| Ag1 | O3 | 2.710 | **Maximum** | 2.710 |
| Ag3 | O5 | 2.385 | **Minimum** | 2.384 |
| Ag4 | O4 | 2.389 | **Average** | 2.508 |
| Ag5 | O2 | 2.384 | **S.D.** | 0.167 |
| Ag6 | O1 | 2.671 | | |

**Table S8.** O–Ag–Ag and O–Ag–S bond angles corresponding to Fig. S5.

| Atoms | Angle/° | Atoms | Angle/° |
|---|---|---|---|
| O1-Ag6-Ag5 | 61.56 | O4-Ag4-Ag1 | 95.16 |
| O1-Ag6-S2 | 100.22 | O4-Ag4-Ag3 | 126.85 |
| O1-Ag6-S3 | 99.07 | O4-Ag4-Ag5 | 127.13 |
| O2-Ag5-Ag3 | 127.52 | O4-Ag4-S1 | 102.65 |
| O2-Ag5-Ag4 | 128.24 | O4-Ag4-S3 | 102.51 |
| O2-Ag5-Ag6 | 93.81 | O5-Ag3-Ag2 | 96.76 |
| O2-Ag5-S1 | 102.56 | O5-Ag3-Ag4 | 126.00 |
| O2-Ag5-S2 | 101.66 | O5-Ag3-Ag5 | 126.14 |
| O3-Ag1-Ag4 | 61.92 | O5-Ag3-S2 | 102.33 |
| O3-Ag1-S1 | 98.66 | O5-Ag3-S3 | 102.71 |
| O3-Ag1-S2 | 102.61 | | |

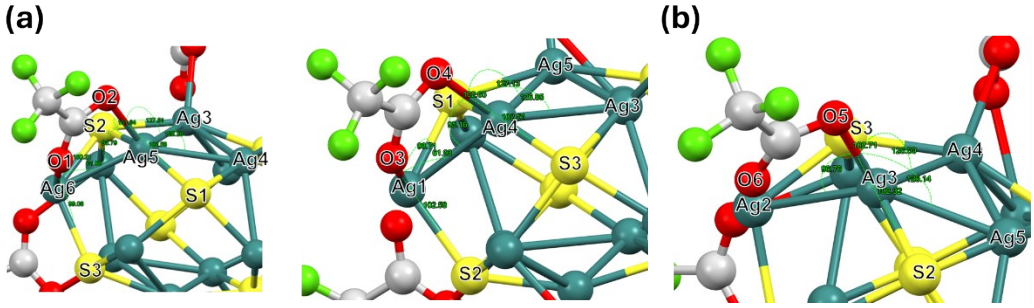

**Fig. S6** Connectivities of (a) four $CF_3COO^-$ ligands with two different Ag atoms by utilizing two O ($\mu_2$-$\eta^1$, $\eta^1$) and (b) the other two $CF_3COO^-$ ligands with one Ag atom by utilizing one O ($\mu_1$-$\eta^1$) in **TUS 6**.

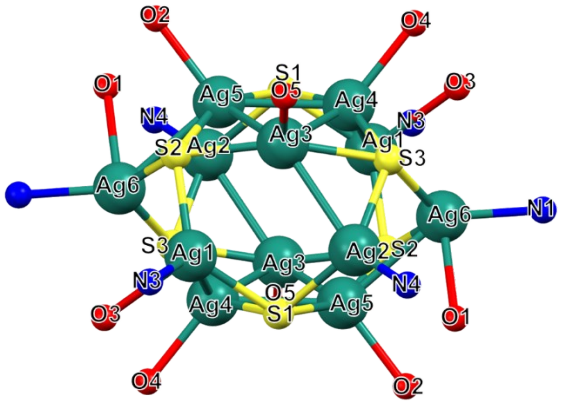


**Fig. S7** Attachment of six linker molecules on the $Ag_{12}S_6O_{10}$ cluster node in **TUS 6**.

**Table S9.** Ag–N bond lengths corresponding to Fig. S7.

| Atom1 | Atom2 | Bond length/Å | | Bond length/Å |
|---|---|---|---|---|
| Ag1 | N3 | 2.279 | **Maximum** | 2.298 |
| Ag2 | N4 | 2.268 | **Minimum** | 2.268 |
| Ag6 | N1 | 2.298 | **Average** | 2.282 |
| | | | **S.D.** | 0.015 |

**Table S10.** N–Ag–Ag, N–Ag–O and N–Ag–S bond angles corresponding to Fig. S7.

| Atoms | Angle/° |
|---|---|
| N1-Ag6-Ag5 | 142.76 |
| N1-Ag6-S2 | 120.74 |
| N1-Ag6-S3 | 117.52 |
| N1-Ag6-O1 | 87.77 |
| N3-Ag1-Ag4 | 142.45 |
| N3-Ag1-S1 | 118.27 |
| N3-Ag1-S2 | 120.51 |
| N3-Ag1-O3 | 87.87 |
| N4-Ag2-Ag3 | 139.95 |
| N4-Ag2-S1 | 120.29 |
| N4-Ag2-S3 | 120.37 |

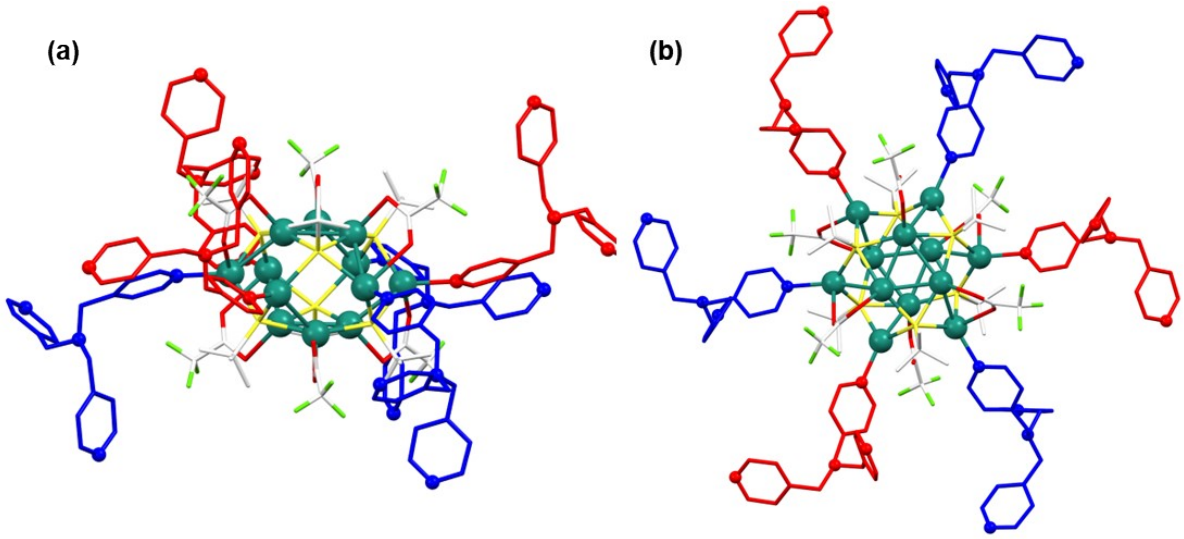


**Fig. S8** The connectivities between $Ag_{12}$ cluster nodes and linkers in **TUS 6** as can be visualized from the (a) side view and (b) top/bottom view.

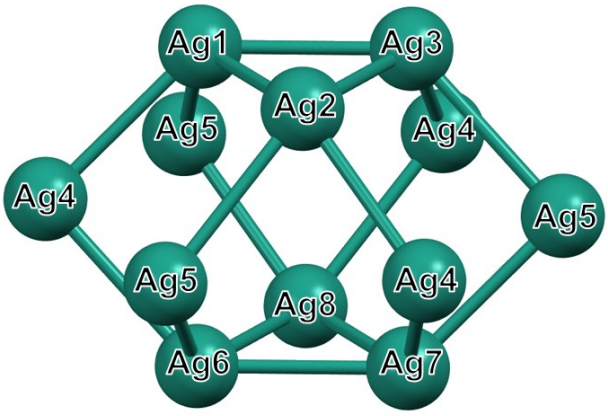


**Fig. S9** $Ag_{12}$ core architecture of **TUS 7**.

**Table S11.** Ag–Ag bond lengths for the $Ag_{12}$ hollow cuboctahedron illustrated in Fig. S9.

| Atom1 | Atom2 | Bond length/Å | | Bond length/Å |
|---|---|---|---|---|
| Ag1 | Ag2 | 3.020 | **Maximum** | 3.228 |
| Ag1 | Ag3 | 3.020 | **Minimum** | 3.02 |
| Ag1 | Ag4 | 3.104 | **Average** | 3.117 |
| Ag1 | Ag5 | 3.228 | **S.D.** | 0.088 |
| Ag2 | Ag3 | 3.020 | | |
| Ag2 | Ag4 | 3.104 | | |
| Ag2 | Ag5 | 3.228 | | |
| Ag3 | Ag4 | 3.104 | | |
| Ag3 | Ag5 | 3.228 | | |
| Ag4 | Ag6 | 3.228 | | |
| Ag4 | Ag7 | 3.228 | | |
| Ag4 | Ag8 | 3.228 | | |
| Ag5 | Ag6 | 3.104 | | |
| Ag5 | Ag7 | 3.104 | | |
| Ag5 | Ag8 | 3.104 | | |
| Ag6 | Ag7 | 3.020 | | |
| Ag6 | Ag8 | 3.020 | | |
| Ag7 | Ag8 | 3.020 | | |

**Table S12.** Ag–Ag–Ag bond angles corresponding to Fig. S9.

| Atoms | Angle/° | Atoms | Angle/° |
|---|---|---|---|
| Ag1-Ag2-Ag3 | 60.00 | Ag6-Ag7-Ag8 | 60.00 |
| Ag1-Ag2-Ag5 | 94.72 | Ag6-Ag7-Ag4 | 94.72 |
| Ag1-Ag3-Ag2 | 60.00 | Ag6-Ag8-Ag7 | 60.00 |
| Ag1-Ag3-Ag4 | 97.71 | Ag6-Ag8-Ag5 | 97.71 |
| Ag2-Ag1-Ag3 | 60.00 | Ag7-Ag6-Ag8 | 60.00 |
| Ag2-Ag1-Ag4 | 97.71 | Ag7-Ag6-Ag5 | 97.71 |
| Ag2-Ag3-Ag5 | 94.72 | Ag7-Ag8-Ag4 | 94.72 |
| Ag3-Ag1-Ag5 | 94.72 | Ag8-Ag6-Ag4 | 94.72 |
| Ag3-Ag2-Ag4 | 97.71 | Ag8-Ag7-Ag5 | 97.71 |

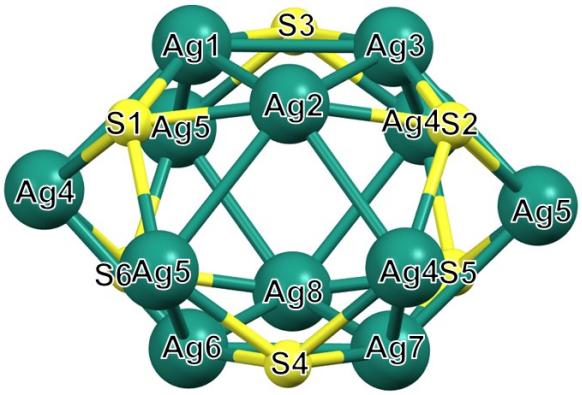


**Fig. S10** Attachment of six thiolates on the $Ag_{12}$ cluster node in **TUS 7**.

**Table S13.** Ag–S bond lengths corresponding to Fig. S10.

| Atom1 | Atom2 | Bond length/Å | Atom1 | Atom2 | Bond length/Å | | Bond length/Å |
|---|---|---|---|---|---|---|---|
| Ag1 | S1 | 2.483 | Ag5 | S1 | 2.509 | **Maximum** | 2.544 |
| Ag1 | S3 | 2.471 | Ag5 | S2 | 2.509 | **Minimum** | 2.471 |
| Ag2 | S1 | 2.471 | Ag5 | S3 | 2.509 | **Average** | 2.519 |
| Ag2 | S2 | 2.483 | Ag5 | S4 | 2.544 | **S.D.** | 0.029 |
| Ag3 | S2 | 2.471 | Ag5 | S5 | 2.544 | | |
| Ag3 | S3 | 2.483 | Ag5 | S6 | 2.544 | | |
| Ag4 | S1 | 2.544 | Ag6 | S4 | 2.544 | | |
| Ag4 | S2 | 2.544 | Ag6 | S6 | 2.544 | | |
| Ag4 | S3 | 2.544 | Ag7 | S4 | 2.544 | | |
| Ag4 | S4 | 2.509 | Ag7 | S5 | 2.544 | | |
| Ag4 | S5 | 2.509 | Ag8 | S5 | 2.544 | | |
| Ag4 | S6 | 2.509 | Ag8 | S6 | 2.544 | | |

**Table S14.** Ag–S–Ag and Ag–Ag–S bond angles corresponding to Fig. S10.

| Atoms | Angle/° | Atoms | Angle/° | Atoms | Angle/° | Atoms | Angle/° |
|---|---|---|---|---|---|---|---|
| Ag1-S1-Ag2 | 75.12 | Ag5-S4-Ag6 | 76.25 | S3-Ag3-Ag1 | 52.26 | S6-Ag8-Ag6 | 52.26 |
| Ag1-S1-Ag4 | 76.25 | Ag5-S5-Ag7 | 76.25 | S3-Ag3-Ag4 | 52.76 | S6-Ag8-Ag5 | 52.76 |
| Ag1-S3-Ag3 | 75.12 | Ag5-S6-Ag8 | 76.25 | S3-Ag1-Ag3 | 52.63 | S6-Ag6-Ag8 | 52.63 |
| Ag1-S3-Ag5 | 80.84 | Ag6-S4-Ag7 | 75.12 | S3-Ag1-Ag5 | 50.09 | S6-Ag6-Ag4 | 50.09 |
| Ag2-S1-Ag5 | 80.84 | Ag6-S6-Ag8 | 75.12 | S3-Ag4-Ag3 | 50.99 | S6-Ag5-Ag8 | 50.99 |
| Ag2-S2-Ag3 | 75.12 | Ag7-S5-Ag8 | 75.12 | S3-Ag5-Ag1 | 49.07 | S6-Ag4-Ag6 | 49.07 |
| Ag2-S2-Ag4 | 76.25 | S1-Ag1-Ag2 | 52.26 | S4-Ag6-Ag7 | 52.26 | | |
| Ag3-S2-Ag5 | 80.84 | S1-Ag1-Ag4 | 52.76 | S4-Ag6-Ag5 | 52.76 | | |
| Ag3-S3-Ag4 | 76.25 | S1-Ag2-Ag1 | 52.63 | S4-Ag7-Ag6 | 52.63 | | |
| Ag4-S1-Ag5 | 94.31 | S1-Ag2-Ag5 | 50.09 | S4-Ag7-Ag4 | 50.09 | | |
| Ag4-S2-Ag5 | 94.31 | S1-Ag4-Ag1 | 50.99 | S4-Ag5-Ag6 | 50.99 | | |
| Ag4-S3-Ag5 | 94.31 | S1-Ag5-Ag2 | 49.07 | S4-Ag4-Ag7 | 49.07 | | |
| Ag4-S4-Ag5 | 94.31 | S2-Ag2-Ag3 | 52.26 | S5-Ag7-Ag8 | 52.26 | | |
| Ag4-S4-Ag7 | 80.84 | S2-Ag2-Ag4 | 52.76 | S5-Ag7-Ag5 | 52.76 | | |
| Ag4-S5-Ag5 | 94.31 | S2-Ag3-Ag2 | 52.63 | S5-Ag8-Ag7 | 52.63 | | |
| Ag4-S5-Ag8 | 80.84 | S2-Ag3-Ag5 | 50.09 | S5-Ag8-Ag4 | 50.09 | | |
| Ag4-S6-Ag5 | 94.31 | S2-Ag4-Ag2 | 50.99 | S5-Ag5-Ag7 | 50.99 | | |
| Ag4-S6-Ag6 | 80.84 | S2-Ag5-Ag3 | 49.07 | S5-Ag4-Ag8 | 49.07 | | |

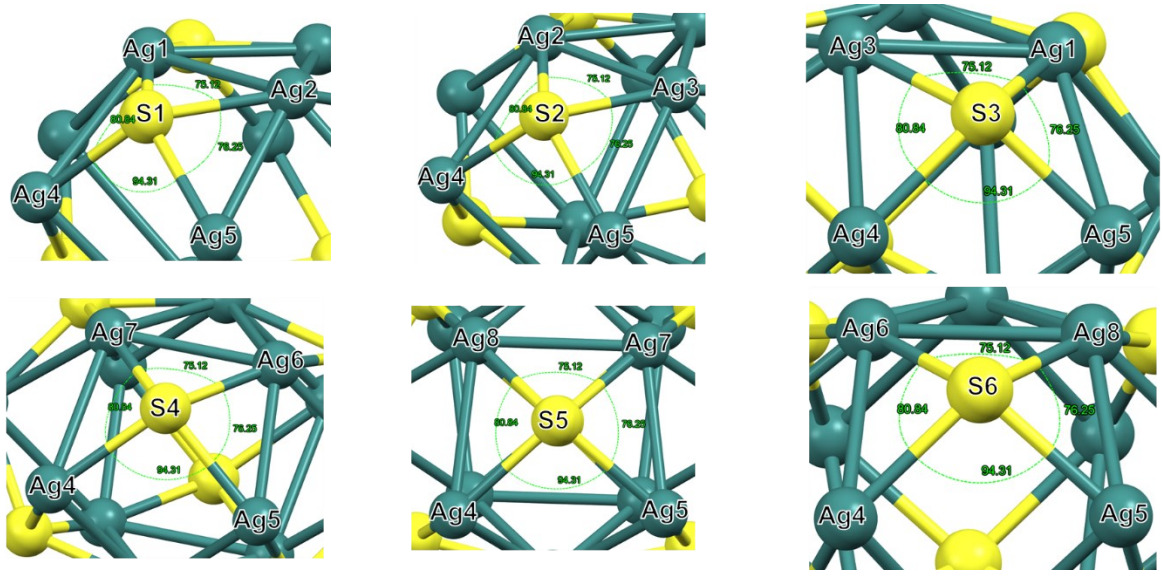


**Fig. S11** Connectivities of six S atoms that belong to S$^t$Bu molecules and constructing the cluster nodes with four different Ag atoms in $\mu_4$-$\eta^1$, $\eta^1$, $\eta^1$, $\eta^1$ ligation in **TUS 7**.

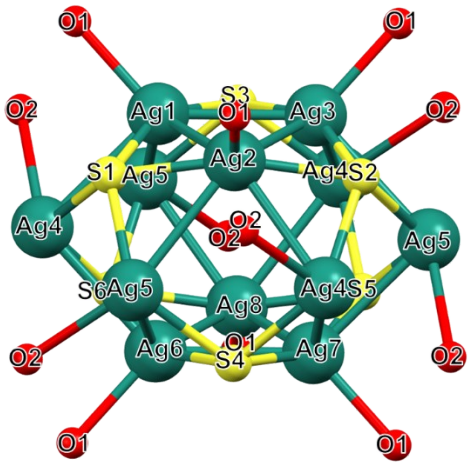


**Fig. S12** Attachment of six trifluoroacetates on the $Ag_{12}S_6$ cluster node in **TUS 7**.

**Table S15.** Ag–O bond lengths corresponding to Fig. S12.

| Atom1 | Atom2 | Bond length/Å | | Bond length/Å |
|---|---|---|---|---|
| Ag1 | O1 | 2.401 | **Maximum** | 2.684 |
| Ag2 | O1 | 2.401 | **Minimum** | 2.401 |
| Ag3 | O1 | 2.401 | **Average** | 2.472 |
| Ag4 | O2 | 2.684 | **S.D.** | 0.131 |
| Ag5 | O2 | 2.684 | | |
| Ag6 | O1 | 2.401 | | |
| Ag7 | O1 | 2.401 | | |
| Ag8 | O1 | 2.401 | | |

**Table S16.** O–Ag–Ag and O–Ag–S bond angles corresponding to Fig. S12.

| Atoms | Angle/° | Atoms | Angle/° | Atoms | Angle/° | Atoms | Angle/° | Atoms | Angle/° |
|---|---|---|---|---|---|---|---|---|---|
| O1-Ag1-Ag2 | 130.84 | O1-Ag3-Ag1 | 95.16 | O2-Ag4-S2 | 98.50 | O2-Ag5-S1 | 96.56 | O1-Ag7-Ag8 | 130.84 |
| O1-Ag1-Ag3 | 131.91 | O1-Ag3-Ag2 | 126.85 | O2-Ag4-S4 | 96.56 | O2-Ag5-S4 | 98.50 | O1-Ag7-Ag6 | 131.91 |
| O1-Ag1-Ag4 | 92.80 | O1-Ag3-Ag4 | 127.13 | O2-Ag4-Ag3 | 61.28 | O2-Ag5-Ag3 | 139.38 | O1-Ag7-Ag4 | 96.12 |
| O1-Ag1-Ag5 | 96.12 | O1-Ag3-Ag5 | 102.65 | O2-Ag4-Ag8 | 139.38 | O2-Ag5-Ag7 | 61.28 | O1-Ag7-Ag5 | 92.80 |
| O1-Ag1-S1 | 102.33 | O1-Ag3-S3 | 102.51 | O2-Ag4-S3 | 98.50 | O2-Ag5-S2 | 96.56 | O1-Ag7-S5 | 102.33 |
| O1-Ag1-S3 | 103.68 | O1-Ag3-S2 | 96.76 | O2-Ag4-S5 | 96.56 | O2-Ag5-S5 | 98.50 | O1-Ag7-S4 | 103.68 |
| O1-Ag2-Ag3 | 130.84 | O2-Ag4-Ag1 | 61.28 | O2-Ag5-Ag1 | 139.38 | O1-Ag6-Ag7 | 130.84 | O1-Ag8-Ag6 | 130.84 |
| O1-Ag2-Ag1 | 131.91 | O2-Ag4-Ag6 | 139.38 | O2-Ag5-Ag6 | 61.28 | O1-Ag6-Ag8 | 131.91 | O1-Ag8-Ag7 | 131.91 |
| O1-Ag2-Ag4 | 92.80 | O2-Ag4-S1 | 98.50 | O2-Ag5-S3 | 96.56 | O1-Ag6-Ag4 | 96.12 | O1-Ag8-Ag4 | 96.12 |
| O1-Ag2-Ag5 | 96.12 | O2-Ag4-S6 | 96.56 | O2-Ag5-S6 | 98.50 | O1-Ag6-Ag5 | 92.80 | O1-Ag8-Ag5 | 92.80 |
| O1-Ag2-S2 | 102.33 | O2-Ag4-Ag2 | 61.28 | O2-Ag5-Ag2 | 139.38 | O1-Ag6-S4 | 102.33 | O1-Ag8-S6 | 102.33 |
| O1-Ag2-S1 | 103.68 | O2-Ag4-Ag7 | 139.38 | O2-Ag5-Ag6 | 61.28 | O1-Ag6-S6 | 103.68 | O1-Ag8-S5 | 103.68 |

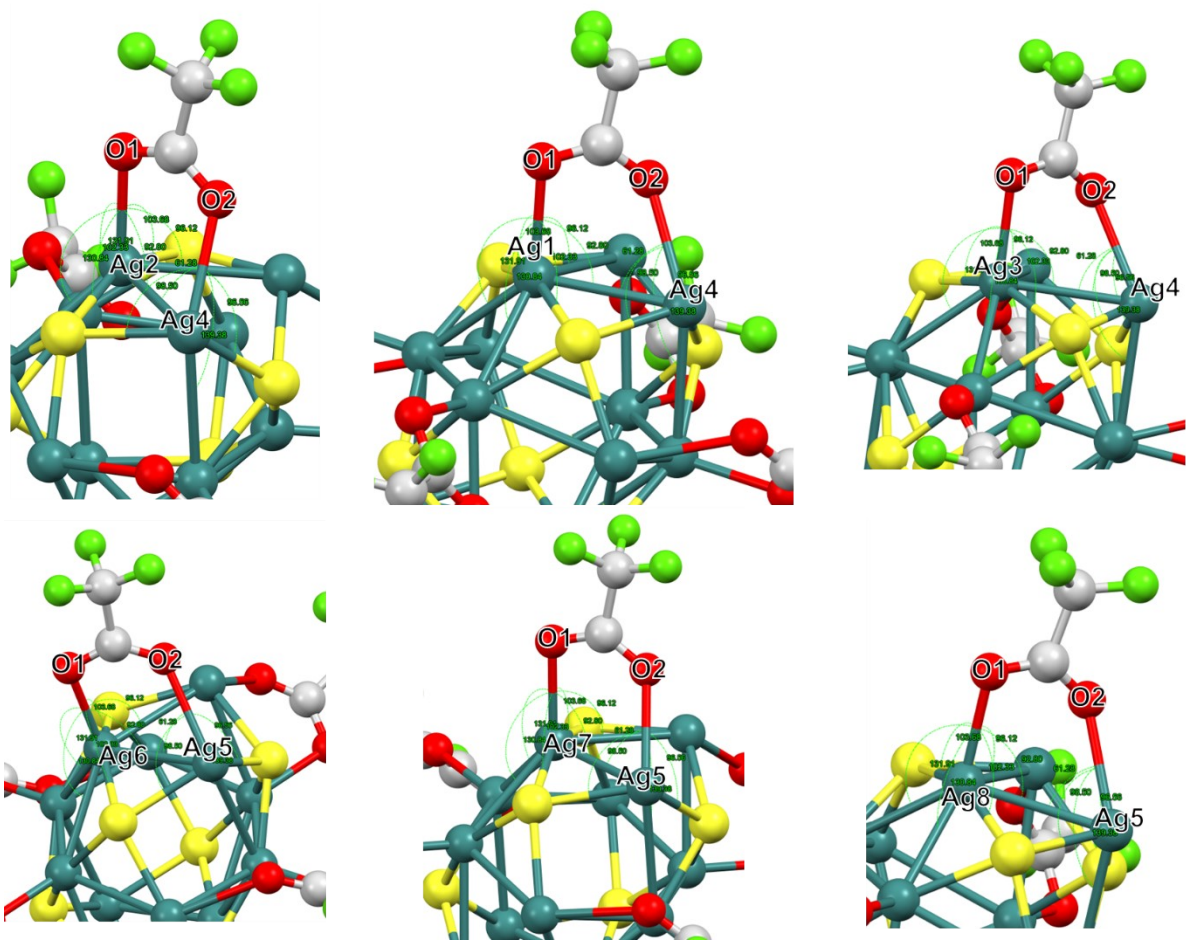


**Fig. S13** Connectivities of $CF_3COO^-$ ligands with two different Ag atoms by utilizing two O ($\mu_2$-$\eta^1$, $\eta^1$) in **TUS 7**.

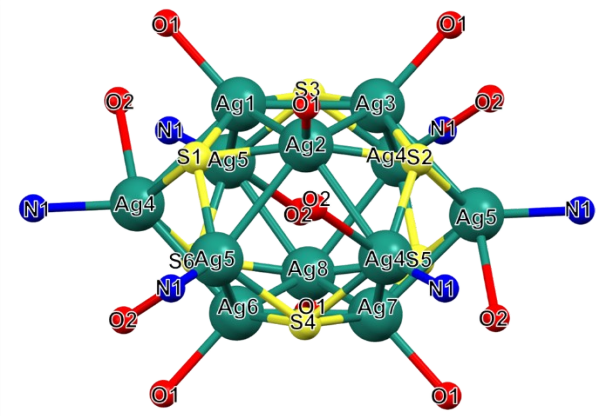


**Fig. S14** Attachment of six linker molecules on the $Ag_{12}S_6O_{12}$ cluster node in **TUS 7**.

**Table S17.** Ag–N bond lengths corresponding to Fig. S14.

| Atom1 | Atom2 | Bond length/Å | | Bond length/Å |
|---|---|---|---|---|
| Ag4 | N1 | 2.275 | **Maximum** | 2.275 |
| Ag5 | N1 | 2.275 | **Minimum** | 2.275 |
| | | | **Average** | 2.275 |
| | | | **S.D.** | 0.000 |

**Table S18**. N–Ag–Ag, N–Ag–O and N–Ag–S bond angles corresponding to Fig. S14.

| Atoms | Angle/° | Atoms | Angle/° | Atoms | Angle/° |
|---|---|---|---|---|---|
| N1-Ag4-Ag1 | 137.87 | N1-Ag5-Ag1 | 129.22 | N1-Ag4-O2 | 85.22 |
| N1-Ag4-Ag2 | 137.87 | N1-Ag5-Ag2 | 129.22 | N1-Ag5-O2 | 85.22 |
| N1-Ag4-Ag3 | 137.87 | N1-Ag5-Ag3 | 129.22 | | |
| N1-Ag4-Ag6 | 129.22 | N1-Ag5-Ag6 | 137.87 | | |
| N1-Ag4-Ag7 | 129.22 | N1-Ag5-Ag7 | 137.87 | | |
| N1-Ag4-Ag8 | 129.22 | N1-Ag5-Ag8 | 137.87 | | |
| N1-Ag4-S1 | 117.65 | N1-Ag5-S1 | 123.04 | | |
| N1-Ag4-S2 | 117.65 | N1-Ag5-S2 | 123.04 | | |
| N1-Ag4-S3 | 117.65 | N1-Ag5-S3 | 123.04 | | |
| N1-Ag4-S4 | 123.04 | N1-Ag5-S4 | 117.65 | | |
| N1-Ag4-S5 | 123.04 | N1-Ag5-S5 | 117.65 | | |
| N1-Ag4-S6 | 123.04 | N1-Ag5-S6 | 117.65 | | |

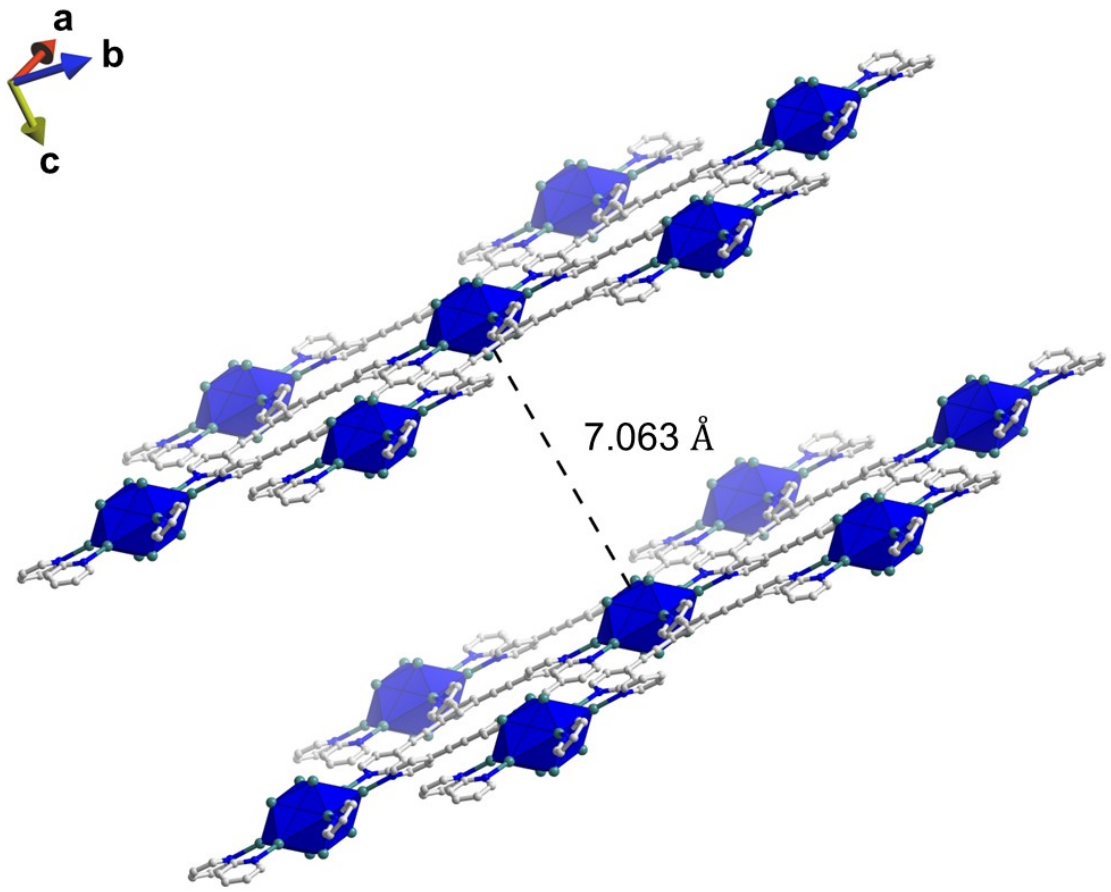


**Fig. S15** The layer distance between the structure of **TUS 7**.

| Atom No. | $Ag_8$ cuboid core $Ag_{12}$ NC | $Ag_6$ middle layer TUS 6 | TUS 7 |
|---|---|---|---|
| 1 | Ag5 | Ag6 | Ag4 |
| 2 | Ag5 | Ag6 | Ag4 |
| 3 | Ag6 | Ag1 | Ag4 |
| 4 | Ag6 | Ag1 | Ag5 |
| 5 | Ag4 | Ag2 | Ag5 |
| 6 | Ag4 | Ag2 | Ag5 |
| 7 | Ag1 | | |
| 8 | Ag1 | | |

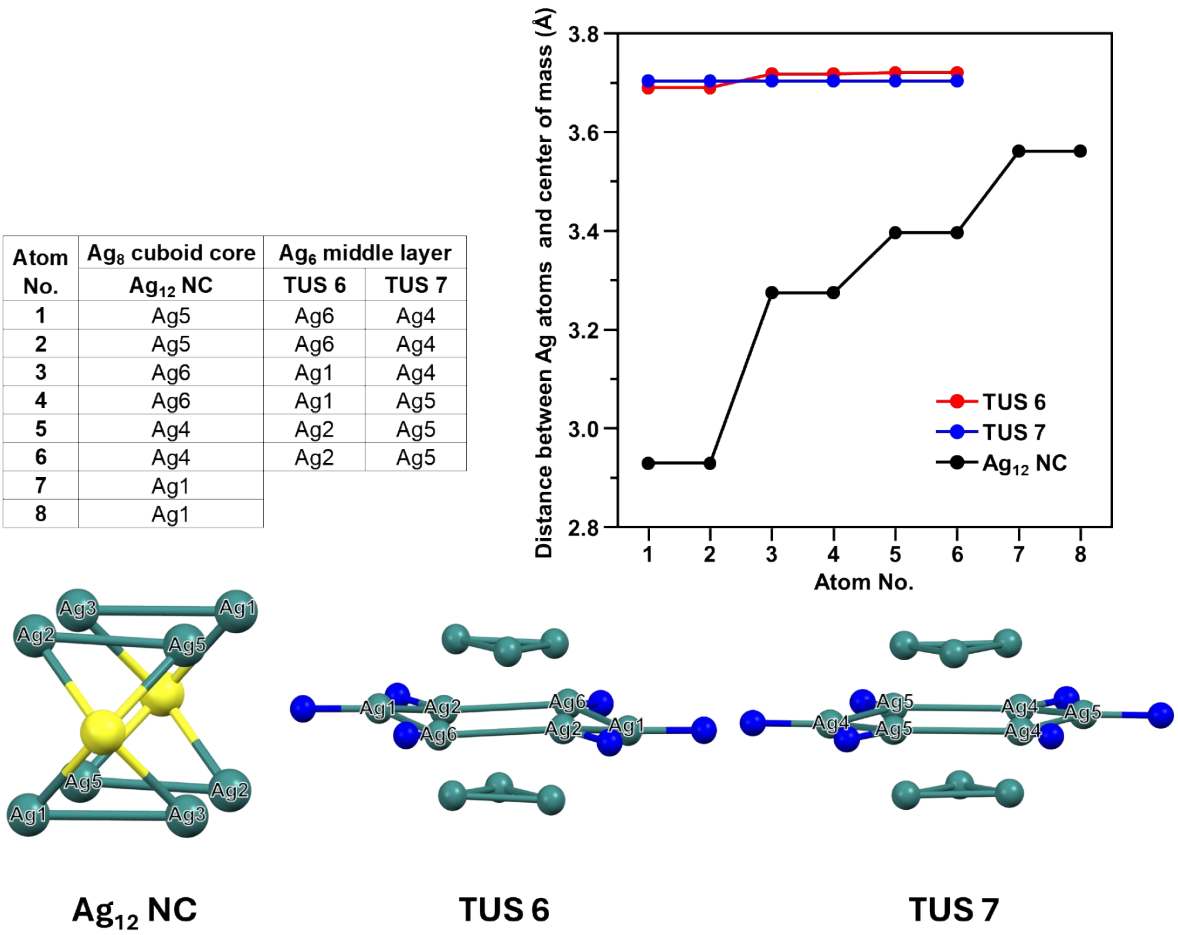


**Fig. S16** $Ag_{12}$ nanocluster symmetry in relation to $Ag_8$ cuboid core versus SCAMs symmetry in relation to $Ag_6$ middle layer.

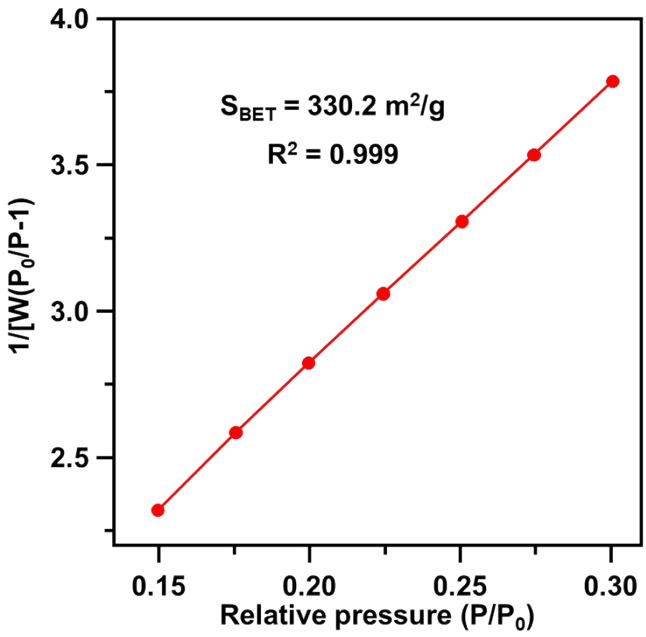


**Fig. S17** BET plot for **TUS 6** calculated from the $N_2$ adsorption isotherms at 77 K.

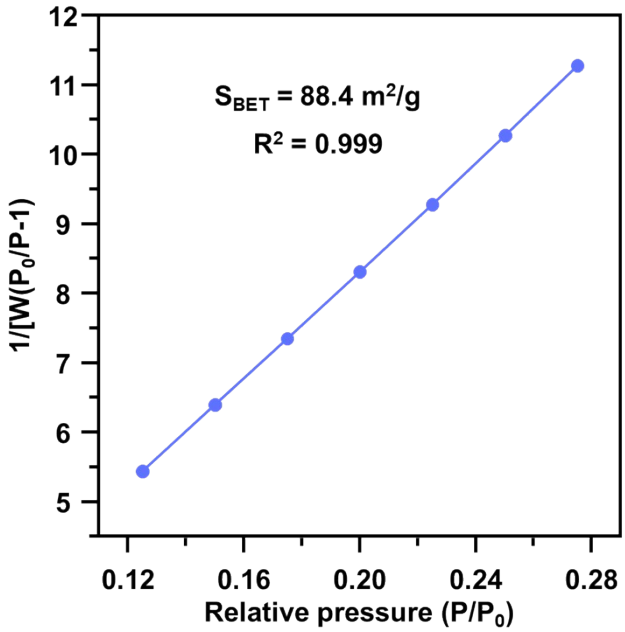


**Fig. S18** BET plot for **TUS 7** calculated from the $N_2$ adsorption isotherms at 77 K.

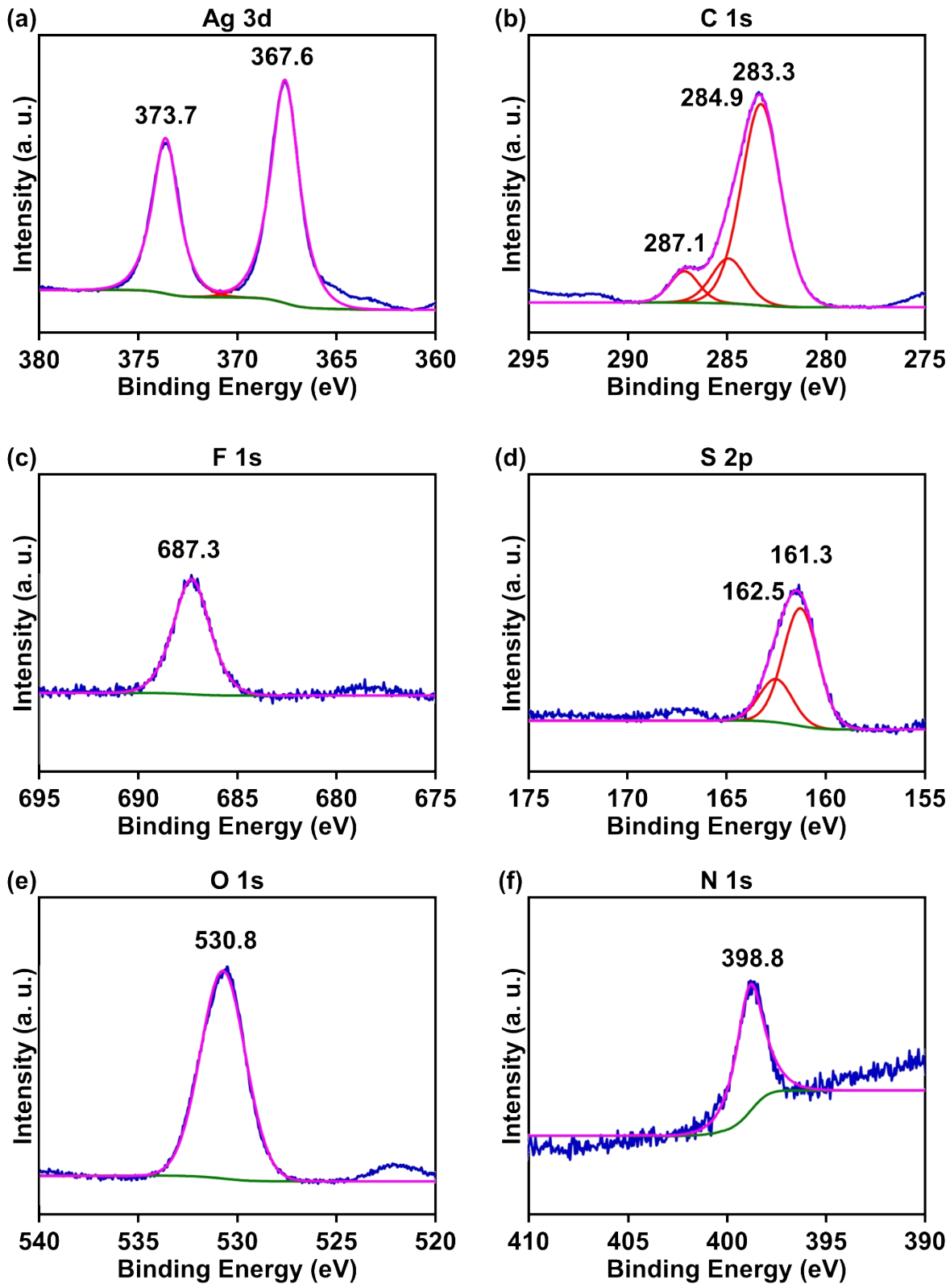


**Fig. S19** High resolution binding energy plot of each element obtained from the XPS measurement of **TUS 6**.

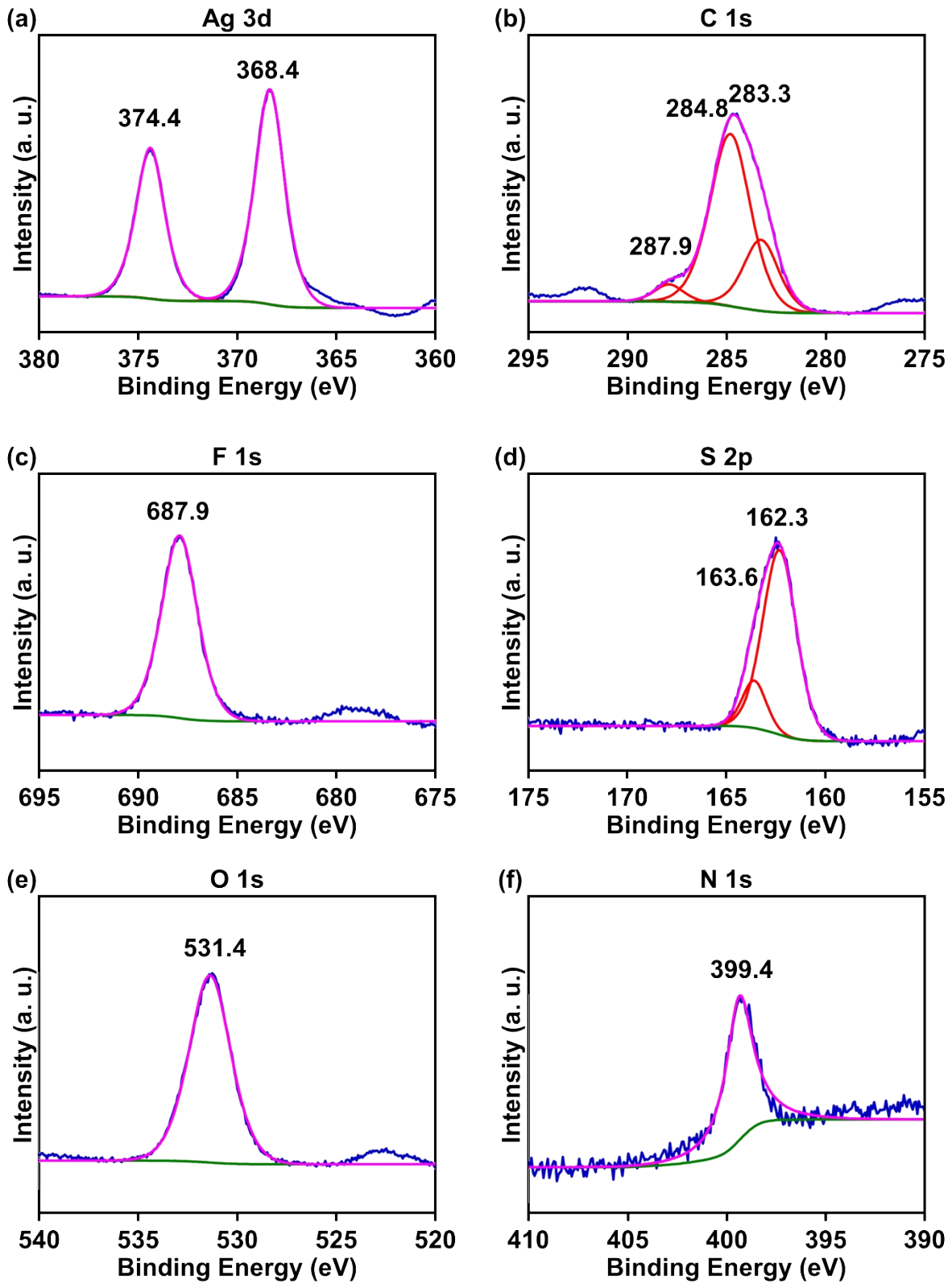


**Fig. S20** High resolution binding energy plot of each element obtained from the XPS measurement of **TUS 7**.

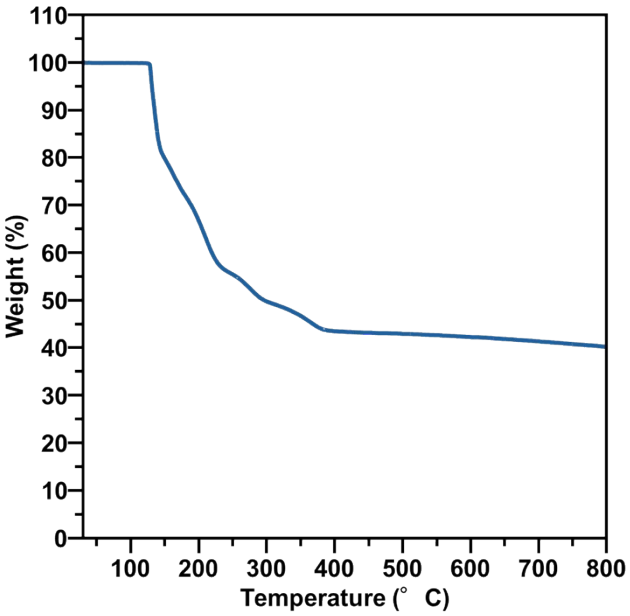


**Fig. S21** TGA curve of **TUS 6** under $N_2$ atmosphere.

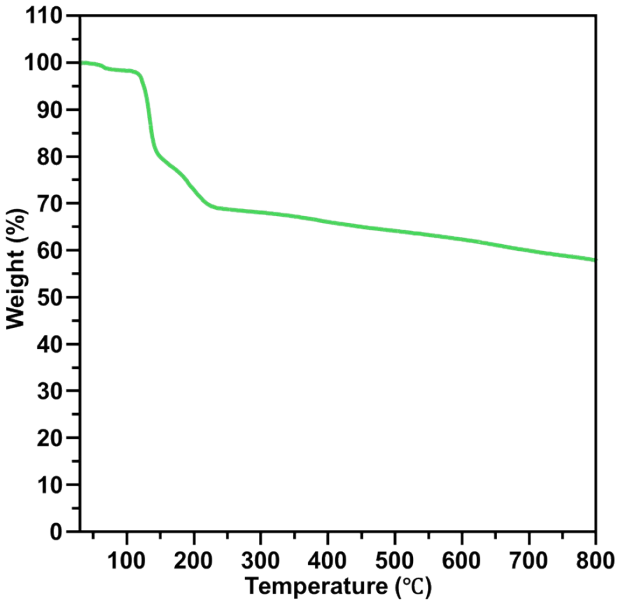


**Fig. S22** TGA curve of **TUS 7** under $N_2$ atmosphere.

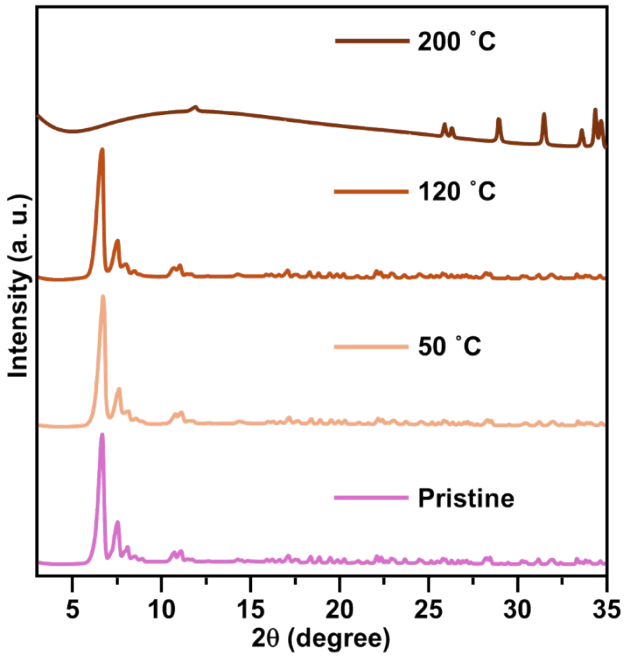


**Fig. S23** PXRD profiles of **TUS 6** after heating at different temperatures.

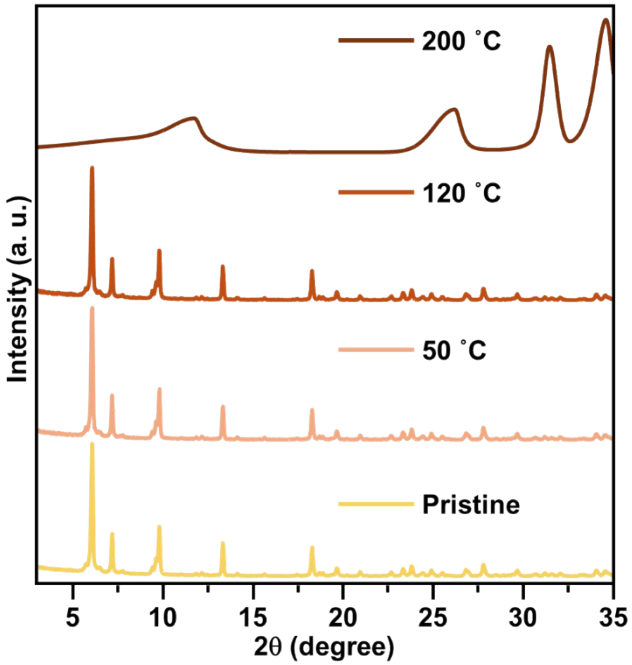


**Fig. S24** PXRD profiles of **TUS 7** after heating at different temperatures.

## References


1. Bruker APEX4, v2019.1–0, Bruker AXS Inc., Madison, WI, USA, 2019.
2. Rigaku Oxford Diffraction, CrysAlisPro software system, version 1.171.40.54. Rigaku Corporation, Oxford, 2019.
3. B. K. Teo, Y. H. Xu, B. Y. Zhong, Y. K. He, H. Y. Chen, W. Qian, Y. J. Deng and Y. H. Zou, *Inorg. Chem.*, 2001, **40**, 6794-6801.
4. S. Das, T. Sekine, H. Mabuchi, S. Hossain, S. Das, S. Aoki, S. Takahashi and Y. Negishi, *Chem. Commun.*, 2023, **59**, 4000-4003.